Proceedings of the ASME 2015 International Mechanical Engineering Congress and Exposition
IMECE2015
November 13-19, 2015, Houston, Texas

IMECE2015-53180

NUMERICAL INVESTIGATION ON THE EFFECT OF ALUMINUM FOAM IN A LATENT THERMAL ENERGY STORAGE

Bernardo Buonomo, Davide Ercole, Oronzio Manca
Dipartimento di Ingegneria Industriale e dell'Informazione,
Seconda Università degli Studi di Napoli,
via Roma 29, 81031 Aversa (CE), Italy

Hasan Celik, Moghtada Mobedi
Department of Mechanical Engineering,
Izmir Institute of Technology,
Urla, Izmir 35430, Turkey

ABSTRACT
In this paper, a numerical investigation on Latent Heat Thermal Energy Storage System (LHTESS) based on a phase change material (PCM) is accomplished. The geometry of the system under investigation is a vertical shell and tube LHTES made with two concentric aluminum tubes. The internal surface of the hollow cylinder is assumed at a constant temperature above the melting temperature of the PCM to simulate the heat transfer from a hot fluid. The other external surfaces are assumed adiabatic. The phase change of the PCM is modeled with the enthalpy porosity theory while the metal foam is considered as a porous media that obeys to the Darcy-Forchheimer law. The momentum equations are modified by adding of suitable source term which it allows to model the solid phase of PCM and natural convection in the liquid phase of PCM. Both local thermal equilibrium (LTE) and local thermal non-equilibrium (LTNE) models are examined. Results as a function of time for the charging phase are carried out for different porosities and assigned pore per inch (PPI).
The results show that at high porosity the LTE and LTNE models have the same melting time while at low porosity the LTNE has a larger melting time. Moreover, the presence of metal foam improves significantly the heat transfer in the LHTES giving a very faster phase change process with respect to pure PCM, reducing the melting time more than one order of magnitude.

INTRODUCTION
An important natural energy source is given by the sun with important peculiarities such as the absence of environmental pollution, a long term availability and a free energy source. Solar energy source is not continuous and stable and energy storage in a solar power system is a necessary process to align energy conversion with consumer demand. Hence, it is required to install a thermal energy storage (TES) working as a thermal buffer which allows to store thermal energy when acquirable and release it when there are energy source lacks. Another important aspect of TES is to prevent also the micro-pauses and the energy supply intermittences, even for short times. In such way, the system thermal inertia increases allowing to avoid continuous service gaps.
There are three types of thermal energy storage systems (TESS): chemical energy storage system (CESS), sensible heat thermal energy storage system (SHTESS) and latent heat thermal energy storage system (LHTESS). The first system stores the heat through reversible chemical reactions, so when it receives heat the behavior of the chemical process is endothermic and when it releases heat the chemical process is exothermic [1]. The second system is based on increasing the temperature of the material that the system is made. The third system uses the phase change materials (PCMs) to store thermal energy at quasi-constant temperature. During the phase change process, the heat is used to change phase and not to increase the temperature [2]. The LHTESS presents many advantages such as high energy density, constant temperature and stability. It is possible to have three type of transformation: solid-solid phase change process, solid-liquid phase change process and liquid-gas phase change process [3].
Recently, TES is receiving a very large attention due to the huge applications, as shown in [1-22]. The solid-liquid phase change process is better than two other processes because it represents the best compromise between solid-solid and liquid-gas phase change and it has a remarkable value of latent heat of fusion and a small volume variation. The use of PCMs allows to increase the energy efficiency because it gives the possibility of storing energy at a quasi-constant temperature with very high energy stored density values and stability. Moreover, one of the main aims is sizing and optimizing the LHTESS in order to

achieve the best possible solution taking into account also the thermal energy charge and discharge times in the storage.

Often, the PCM is an organic material, such as paraffin, and it is not corrosive; the process of phase change is congruent without segregation of the material and nontoxic [23]. Nevertheless, the worse drawback of this material is the small value of the thermal conductivity, which requires a long time for melting and a broad difference of temperature in the system between the solid zone and liquid zone. To cover such inconvenience, a wide range of ameliorative solutions has been implemented to improve the rate of melting: finned tubes [24], metal foam [25] and injection of nanoparticles into PCM [26]. In particular, using of the open-cell metal foams improves the effective thermal conductivity of the whole system, because they have a large area of heat exchange and the base material has a high value of conductivity [27].

Krishnan et al. [28] studied numerically the phase change in a rectangular enclosure filled with a metal foam impregnated with PCM in local thermal non-equilibrium (LTNE) assumption. Siahpush et al. [29] accomplished an experimental and analytical investigation to determine copper porous foam effect on the heat transfer performance enhancement in a cylindrical solid/liquid phase change thermal energy storage system. The model was developed in local thermal equilibrium (LTE) assumption. Zhao et al. [25] investigated experimentally the solid/liquid phase change heat transfer in a copper foam with PCM, a paraffin wax RT58, in order to examine the usability of metal foams to enhance the heat transfer capability of PCM in the low-temperature thermal energy storage systems. Moreover, they developed also a two-dimensional numerical model in LTNE comparing the predicted results with the experimental data. An experimental investigation on copper foam with paraffin RT27 was carried out [30]. A two dimensional model on copper foam with paraffin RT58 in LTNE assumption was studied numerically in [31]. A comparison among PCM (sodium nitrate) in different metal foams or expanded graphite in a cylindrical tank was performed experimentally by Zhao and Wu [32]. An experimental study examining the heat charging process were carried out in [33] considering two conditions: paraffin filled with and without copper foam. A three-dimensional model to simulate a thermal energy storage system with PCM in metal foam and fins was presented in [34]. The natural convection in the liquid part of PCM was considered and volume-averaged mass and momentum equations were employed with the Brinkman–Forchheimer extension to Darcy law to simulate the porous resistance. A local thermal equilibrium model was developed to obtain temperature field. A numerical model to evaluate the PCM melting process in aluminum foam was developed in [35]. The heat transfer enhancement by means of metal foam in a shell-and-tube LHTES unit was studied. A numerical analysis on the pore size and porosity effect on the performance of PCM in microcellular aluminum foams was performed in [36]. A three dimensional finite element model was developed to study in LTNE. An experimental and numerical investigation on thermal energy storage with $NaNO_3/KNO_3$-PCM was presented in [37]. Results for a heat storage application with PCM tubular heat exchanger and metallic foam and metallic sponge to increase the effective thermal conductivity of the PCM were also considered. An experimental study on the melting behavior of PCM, paraffin wax, in aluminum foams was carried out at the pore scale in [38]. Moreover, a two dimensional numerical lattice Boltzmann model was also developed. The numerical results agree well with the experimental observations qualitatively. Xiao et al. [39] experimentally investigated the effect of open-cell metal foams embedded with pure paraffin. They concluded that the effective thermal conductivity was enhanced drastically by using metal foams in relation to the pure paraffin.

A passive thermal management system for high powered lithium-ion battery packs using a sandwich structure combined with a PCM, paraffin, in copper foam was designed and experimentally investigated in [40]. A three-dimensional numerical model for a PCM in a heat sink with aluminum metal foam and crossed fins was provided in [41]. The porosity and the pores per inch of the foam were varied and natural convection were investigated. A cylindrical LTES component with eutectic salt (50 wt% $NaNO_3$, 50 wt% KNO_3) in two different metal foams (copper foam and nickel foam) were experimentally and numerically investigated by Zhang et al. [42]. Moreover, a three-dimensional model assuming the LTNE between the salt and metal foam was developed to evaluate the heat transfer behaviors. The melting process of paraffin in aluminum foam and its cooling effect on Li-ion batteries was experimentally studied in [43]. The effect of the addition of aluminum foam on temperature uniformity along different directions and the heat storage rate of the PCM was discussed. A numerical study on melting behavior of PCM in a copper foam was carried out in [44]. The effect of porosity was considered and the results showed an heat transfer enhancement during thermal energy storage and the optimization of porous media structure was found. The melting process and heat transfer behaviors of a porous medium filled with nano-PCM in an enclosure heated from the side was investigated analytically and numerically in [45]. A numerical analysis on three configurations of a thermal energy storage system with PCM was accomplished in [46]. The three configurations were made with pure PCM, with PCM in aluminum foam and with PCM in aluminum meshes. Moreover, a comparison between the configuration with aluminum foam and experimental data was provided.

After the short review it seems to the authors' knowledge that there is a lack of information on numerical model in TES with PCM inside metal foams for a cylindrical geometry during the charging and discharging phases. It is important to provide information on thermal behaviors of this configuration in transient regime for a vertical coaxial cylinders configuration of a LHTES and evaluate the differences in terms of LTE and LTNE models. In this paper a LHTESS, in which aluminum foam is embedded with paraffin wax as PCM, is numerically investigated in two-dimensional model. The process of phase change is modeled with enthalpy-porosity method [47]. Darcy-

Forchheimer law is employed for the metal foam part. Local thermal equilibrium (LTE) and local thermal non-equilibrium (LTNE) in term of melting time for metal foam is investigated and presented in this study.

GEOMETRICAL AND PHYSICAL MODELS

The geometry considered for the LHTES system is a vertical shell tube with two concentric aluminum tubes, as shown in Fig. 1. The length of the cylindrical system is 100 mm, the inner radius is 2 mm and outer radius is 12 mm, as reported in Fig. 2a. The domain is two-dimensional and the condition of axial symmetry is considered. The gravitational acceleration is along the vertical x-axis and the PCM with metal foam are included between the two cylindrical tubes as shown in Fig. 1. In the simulation, the inner surface is at a constant temperature T equal to 350 K while the other surfaces are assumed adiabatic, as shown in Fig. 2b.

There are two methods, which can be used to simulate the melting and solidification of PCM as the temperature-based and enthalpy-based methods [48]. In the first method, there are two energy equations both solid phase and liquid phase of PCM, the solid-liquid interface position is known and marked. In the second method, the solid-liquid interface position is not explicitly known but there is a mixed solid-liquid phase zone that is described as a "pseudo" porous zone where the porosity is the liquid fraction, which indicates the fraction of liquid form in a cell of the mixed zone [48]. The value of the liquid fraction, β, is 0 when the zone is fully solid, 1 when it is fully liquid and between 0 to 1 in the mushy zone:

$$\begin{cases} \beta = 0 & \text{for} \quad T < T_{solidus} \\ \beta = \dfrac{T - T_{solidus}}{T_{liquidus} - T_{solidus}} & \text{for} \quad T_{solidus} < T < T_{liquidus} \\ \beta = 1 & \text{for} \quad T > T_{liquidus} \end{cases} \tag{1}$$

where T is the temperature and $T_{solidus}$ and $T_{liquidus}$ are the solid and liquid phase temperatures. The PCM melts in a range of temperature, where $T_{liquidus}$ represents the temperature upper which every part of the PCM is in a liquid phase and $T_{solidus}$ is the temperature below which the PCM is fully solid. The solid-liquid mixture zone exists in a range of temperature between $T_{liquidus}$ and $T_{solidus}$.

A source term is added to the momentum equation to take account the presence of the solid zone. To assess the pressure drop caused by the porous media (i.e. metal foam), another source term is used in the momentum equation. Two models are considered to evaluate the heat transfer between PCM and porous media. The first model is the Local Thermal Equilibrium (LTE) assumption, it considers the PCM and porous media at the same temperature. The second model is Local Thermal Non-Equilibrium (LTNE) assumption, where porous media and PCM are not in thermal equilibrium and two energy equations should be written, one for PCM and other for porous zone [35].

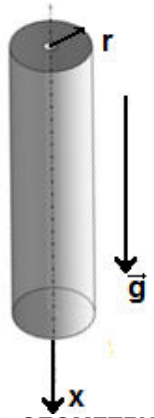

FIGURE 1. GEOMETRY OF THE LHTES SYSTEM CONSIDERED.

The hypothesis in the present study are the following:

1) The physical domain is a two-dimensional vertical annular domain confined by two coaxial cylinders.
2) The metal foam is isotropic and homogenous.
3) The variation of density in the liquid PCM follows the Boussinesq approximation.
4) The other proprieties of PCM are assumed constant.
5) The boundary condition of the internal surface is an isothermal surface.

According to the second hypothesis, to simulate the natural convection in the PCM a Boussinesq approximation is used, so the density of PCM varies with temperature:

$$\rho = \rho_0[1 - \gamma(T - T_0)] \tag{2}$$

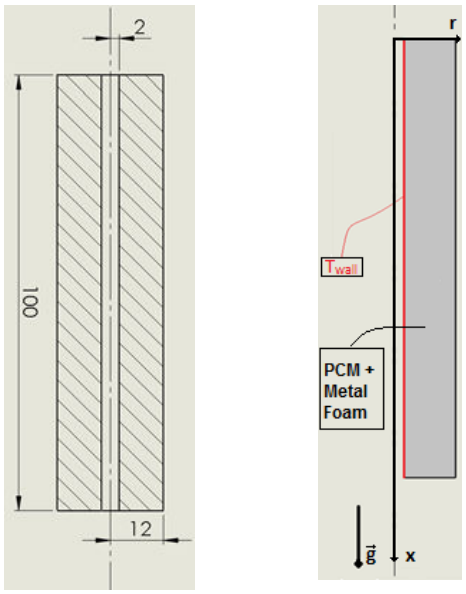

(a) **(b)**

FIGURE 2. SKETCH OF DOMAIN: (A) DIMENSIONS; (B) COMPUTATIONAL DOMAIN AND BOUNDARY CONDITIONS.

where ρ and T are respectively the density and the temperature of the PCM, ρ_0 and T_0 are the operating density and temperature and γ is the thermal expansion coefficient.
The continuity equation is:

$$\nabla \cdot (\rho \vec{V}) = 0 \tag{3}$$

where $\vec{V}$ is the velocity vector of the PCM liquid phase.
The momentum equation is [49]:

$$\rho\left(\frac{\partial \vec{V}}{\partial t} + \left(\nabla \cdot \vec{V}\right)\vec{V}\right) = \mu\left(\nabla^2 \vec{V}\right) - \nabla \vec{p} + \vec{S} \tag{4}$$

Where μ is the viscosity of the PCM, p is the pressure and vector $\vec{S}$ is a source term given as [49]:

$$\vec{S} = \frac{(1-\beta)^2}{\left(\beta^3 + \pi\right)^3} A_{mush}\vec{V} + \frac{\mu}{K}\vec{V} + \frac{C_F}{\sqrt{K}}\rho\vec{V}\left|\vec{V}\right| + \rho\vec{g}\gamma\left(T - T_0\right) \tag{5}$$

The first term on the right side models the presence of the solid part in the mixed region. In fact, β is the liquid fraction, π is a small number (0.001) to avoid division by zero [49], A_{mush} is the mushy zone constant which represents the damping of the velocity to zero during the solidification [48]. The second term is the Darcy term where K is the permeability of the porous media; the third term is the Forchheimer term, where C_F is inertial drag factor. The last term on the right side of equation (5) is the buoyancy effect.
The energy conservation equation for LTE model is, [35]:

$$\overline{\rho c}\frac{DT}{Dt} = k_{eff}\nabla^2 T - \varepsilon\rho_{pcm}H_L\frac{\partial \beta}{\partial t} \tag{6}$$

where the product $\overline{\rho c}$ is calculated, [35]:

$$\overline{\rho c} = (1-\varepsilon)\rho_m c_m + \varepsilon\rho_{pcm}c_{pcm} \tag{7}$$

where ρ_m and c_m are respectively the density and specific heat of the metal foam, ε is the porosity of the metal foam and c_{pcm} is the specific heat of PCM. k_{eff} is the effective thermal conductivity calculated as the weighted average of the conductivities of metal foam and PCM, [35]:

$$k_{eff} = (1-\varepsilon)k_m + \varepsilon k_{pcm} \tag{8}$$

k_m e k_{pcm} are respectively the thermal conductivities of metal foam and PCM. H_L is the latent heat of the PCM and t is the time.
The LTNE model treats the metal and PCM as two distinct elements no longer in thermal equilibrium. Therefore, there are two energy equations, for PCM the conservation energy equation is, [35]:

$$\varepsilon(\rho c)_{pcm}\frac{DT_{pcm}}{Dt} = k_{pcm,eff}\nabla^2 T_{pcm} + h_{sf}\alpha_{sf}\left(T_m - T_{pcm}\right) - \varepsilon\rho_{pcm}H_L\frac{\partial \beta}{\partial t} \tag{9}$$

and for the metal foam is, [35]:

$$(1-\varepsilon)(\rho c)_m\frac{DT_m}{Dt} = k_{m,eff}\nabla^2 T_m + h_{sf}\alpha_{sf}\left(T_{pcm} - T_m\right) \tag{10}$$

Where $k_{pcm,eff}$ and $k_{m,eff}$ are, respectively, the effective thermal conductivity of the PCM and metal foam. The calculation of these parameters is described in Boomsma et al. [50]; h_{sf} is the local heat transfer coefficient, α_{sf} is the surface area density of the metal foam, T_{pcm} is the PCM temperature and T_m is the metal foam temperature. In this model T_{pcm} and T_m are not equal and the heat transfer from metal foam to PCM occurs through the product $h_{sf}\,\alpha_{sf}$.
Enthalpy-porosity method is used for the modeling of the PCM, with a value A_{mush} of 10^5 [48].The effect of the A_{mush} on the melting time is analyzed and it is concluded that there is not a correlation with the presence of the metal foam; the time of melting is the same to values from 10^4 to 10^9 as shown in Fig. 3. The chosen material is the paraffin RT58 of the Rubitherm [51] and the properties are listed in Table 1. In the Boussinesq approximation the operating temperature T_0 is equal to 321 K.
The metal foam considered in the present analysis is an aluminum foam and its thermal properties density, specific heat and thermal conductivity are equal to 2719 kg/m^3, 871 J/kg and 202.4 W/m K, respectively [48]. It behaves as a porous zone that obeys the Darcy-Forchheimer law:

$$\frac{\Delta p}{L} = \frac{\mu}{a}\vec{V} + \rho C_F\vec{V}^2 \tag{11}$$

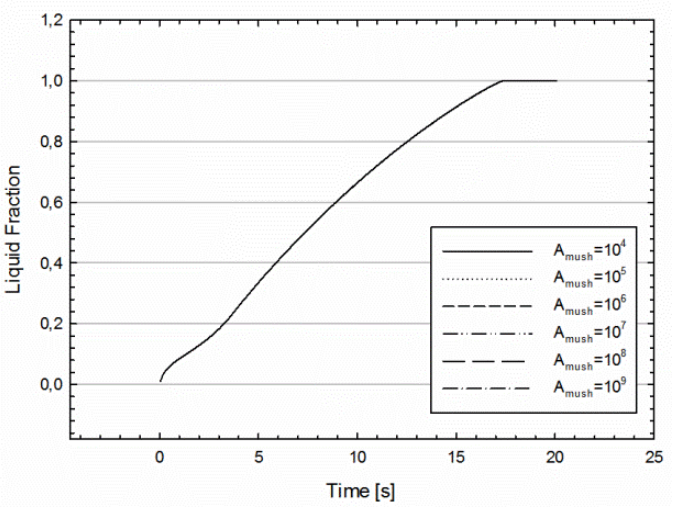

FIGURE 3. LIQUID FRACTION AT VARYING A_{MUSH}

This equation describes the relation between the pressure drop and velocity into porous media for laminar flow. Nevertheless, the permeability and drag factor or inertia coefficient values are assumed the following, [52]:

$$K = 0.00073(1-\varepsilon)^{-0.224}\left(\frac{d_f}{d_p}\right)^{-1.11} d_p^2 \quad (12)$$

$$C_F = 0.00212(1-\varepsilon)^{-0.132}\left(\frac{d_f}{d_p}\right)^{-1.63} \quad (13)$$

where d_f is the ligament diameter of the metal foam, d_p is the pore diameter. This physical characteristics are dependent each other via the following relation [52]:

$$\frac{d_f}{d_p} = 1.18\sqrt{\frac{1-\varepsilon}{3\pi}}\left(\frac{1}{1-e^{1(1-\varepsilon)/0.04}}\right) \quad (14)$$

$$d_p = \frac{0.0224}{\omega} \quad (15)$$

where ω is the pore density of the metal foam that represents the number of pores across one inch. In this study the pore size is assigned at 20 Pore Per Inch (PPI).

The surface area density represents the whole contact area between PCM and metal foam, it is complicated predict both α_{sf} and h_{sf} and for the present study is adopted the following correlation for h_{sf}, [53]:

$$h_{sf} = \begin{cases} \left(0.76 Re_d^{0.4} Pr_{pcm}^{0.37}\right)\left(\frac{k_f}{d_f}\right), & 1 \le Re_d \le 40 \\ \left(0.52 Re_d^{0.5} Pr_{pcm}^{0.37}\right)\left(\frac{k_f}{d_f}\right), & 40 \le Re_d \le 1000 \\ \left(0.26 Re_d^{0.6} Pr_{pcm}^{0.37}\right)\left(\frac{k_f}{d_f}\right), & 1000 \le Re_d \le 2\times10^5 \end{cases} \quad (16)$$

Where Re_d is the local Reynolds number referred to ligament diameter:

$$Re_d = \frac{\rho V d_f}{\mu} \quad (17)$$

and the relation of Calmidi et al. [52] is employed to evaluate α_{sf}:

$$\alpha_{sf} = \frac{3\pi d_f}{\left(0.59 d_p\right)^2}\left(1 - e^{\frac{1(1-\varepsilon)}{0.04}}\right) \quad (18)$$

Table 1: Thermal proprieties of the paraffin RT58

Paraffin RT58 from [51]	Values
Density [Kg/m^3]	840
Specific Heat [J/Kg K]	2100
Thermal Conductivity [W / m K]	0.2
Dynamic Viscosity [Kg/m s]	0.0269
Thermal expansion coefficient [1/K]	0.00011
Melting Heat [J / Kg]	180000
Solidus Temperature [K]	321
Liquidus Temperature [K]	335

Finally, a parameter to evaluate the system efficiency is taken from Yang et al. [34], it represents the energy stored in each time step:

$$q = \frac{E_t - E_{t-\Delta t}}{H_L} \quad (19)$$

Where E_t-$E_{t-\Delta t}$ is the specific enthalpy change in one time step Δt and H_t is the latent heat of fusion of PCM and q is performance parameter. Obviously q is a dimensionless parameter.

3. NUMERICAL MODEL

The commercial CFD code Ansys-Fluent [54] is employed to solve the governing Eqs. (3)-(6) in LTE and Eqs. (3)-(5) and (9), (10) in LTNE. A 2D-axialsymmetric option is also enabled to simulate the phenomenon under investigation. For the pressure-velocity coupling the SIMPLE algorithm is used, for the spatial discretization the gradient evaluation is based on least square cell, the pressure calculation is based on PRESTO, for energy and momentum equation the second order upwind scheme is used. High Order Term Relaxation for only flow variables is set to 0.75. The time step size is fixed at 0.05 s. The residual convergence values are imposed to 10^{-5} for continuity equation and momentum equation while 10^{-8} is set to energy equation. To solve equations (16) and (17), a user-defined functions to link the Reynolds number to the local heat transfer is implemented.

The numerical grid consists of mapped quadrilateral elements with a fine grid near the walls and a coarse grid in the center of the domain. The bias factor is equal to 2 in order to improve the numerical stability. A study to obtain a solution independent from the mesh is made with six different meshes: 4 x 10, 8 x 20, 12 x 30, 16 x 40, 20 x 50 and 40 x 100 nodes. The results in term of melting time are plotted in Fig. 4 and the mesh with 20 x 50 nodes was chosen to carried out the results in this study. It allows to have the right compromise between the numerical accuracy and computational time.

The model is compared with the work of Krishnan et al. [28] for the validation. The same domain, boundary conditions, properties and mesh are used to obtain results to evaluate the model reliability. The results are compared in the Fig. 5 and the two models present a good agreement.

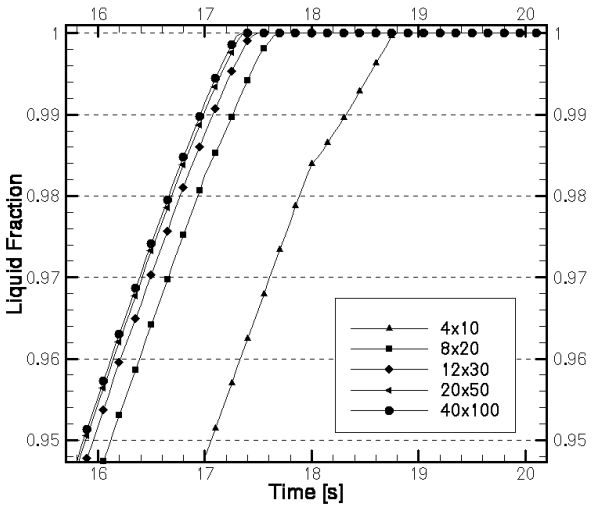

FIGURE 4. INDEPENDENT SOLUTION FROM MESH GRID SIZE

4. RESULTS AND DISCUSSIONS

The results are evaluated employing the LTE and LTNE models with the porosity values ε equal to 0.80, 0.85, 0.90, 0.95, 0.97 and 0.99 at an assigned PPI value equal to 20. In all cases the temperature of the internal cylindrical wall is assumed constant and equal to 350 K and the other surfaces are assumed adiabatic. A comparison in terms of liquid fraction, temperature and performance parameter values is accomplished.

Clean case

In Fig. 6 is shown the evolution of melting for a CLEAN case, without foam at difference time values equal to 30 s,300 s, 900 s, 1500 s and 3000 s. The red zone represents the liquid phase while the blue zone is the solid phase. The other colors represent the mushy zone. The melting time is over 3000 s because of the small value of thermal conductivity of pure PCM. About the shape of melting zone, at the beginning, up to 30 s, it is vertical because of the conduction is predominant with respect to the natural convection. Increasing the time the melt front tends to bend because the natural convection arises and prevails on the heat conduction. Finally, when the domain is nearly melted, the effect of natural convection is completely dominant.

In Fig. 7 the temperature and streamline fields are reported, and it is possible to observe that initially the streamlines are parallel where the conduction is dominant, but as the melting front advances, the streamline begin to incline with it. The behavior of the temperature fields is similar to the melting field; in fact, at the early instants temperature gradients are perpendicular to the melt front because the conduction is predominant while after the trend of field changes significantly.

The mean values of liquid fraction and temperature of the system as functions of time are shown in Fig.8. At the initial times, up to 150 s, the increase of liquid fraction is faster than the one from 150 s to 500 s due to the increase of the musky zone. After 500 s liquid fraction presents a greater increase up

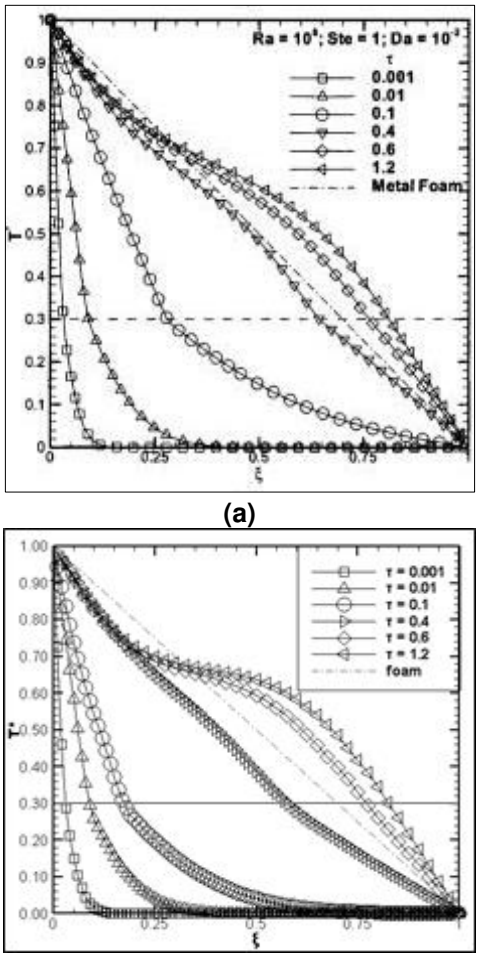

FIGURE 5. COMPARISON WITH THE RESULTS FROM (a) KRISHNAN ET AL. [28] AND (b) PRESENT DATA

to about 2000 s. Mean temperature value at the initial times has a sharp increase up to 600 s and after due to the natural convection effect presents a lower increase.

Case with metal foam in LTE assumption

The liquid fraction distribution, in the domain, together with temperature and streamline fields are presented in Fig. 9 for PCM with metal foam of a porosity equal to 0.80 and 20 PPI. The liquid fraction and temperature fields are considered at t=5 s, 10 s, 12.5 s, 15 s, 20 s whereas the stream function is given at 5 s and the values are very small values (about 10^{-8}kg/s) and the differences for different time values are very small. The results for other porosities present the same qualitative shape of these field, hence they are not reported here for brevity. The liquid fraction fields, in Fig. 9a, show that the melted zone moves uniformly and vertical and the temperature distributions confirm that the conduction is dominant during all the melting.

It is important to observe that the conduction is completely dominant on the overall energy transport because the melt front

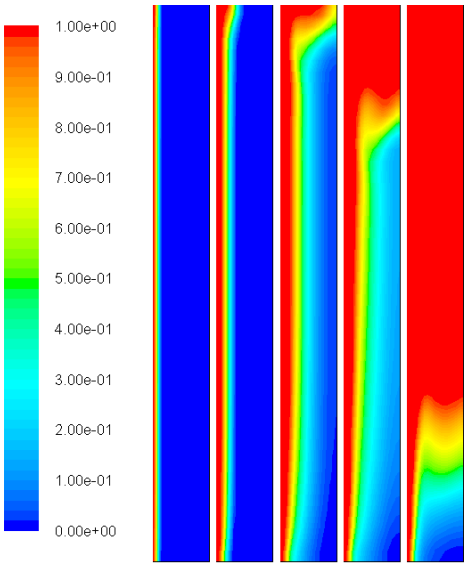

FIGURE 6 LIQUID FRACTION FOR DIFFERENT TIME VALUES (30 s,300 s,900 s,1500 s,3000 s)

is parallel to the heated edge and the time for full melting is very small, more than two order of magnitude with respect of CLEAN case. The presence of the metal foam improves significantly the heat transfer into PCM due to its high value of the thermal conductivity.

In Fig. 10 the average liquid fraction and temperature are reported as functions of time. The average liquid fraction is about a linear function, as shown in Fig. 10a, and the time to obtain a complete melting is reach at t<20 s. Temperature trend can be divided into three different zones as shown in Fig. 10b. In the first zone, the temperature increases very quickly, with a sharp increase, because the melting zone is not developed and the sensible heat is mainly stored. In the second one the melting zone is enlarged in nearly whole domain, and the temperature is nearly constant and the latent heat contributes to the energy storage. Finally, in the third zone the domain is fully melted and the temperature raises up to the T_{wall} value.

In Fig. 11 the thermal performance parameter, q, is plotted as a function of time. At beginning of simulation the q value, Eq. (19), is high because the difference of temperature between the domain and isothermal edge is high and at the same time the sensible heat is prevalent in the storage process. But afterwards the q value decreases rapidly because the high value of the effective thermal conductivity of the system reduces the temperature difference between the isothermal edge and the domain. Moreover, when the melting zone arises and occupies large part of the domain, the steady stage begins and the value of q is nearly constant. In this stage the storage of energy occurs at the nearly constant temperature and the energy stored is the latent heat. The reason for which q is not completely constant depends of the advancing of the melting region whereby the thermal resistance rise slightly. Finally, the q value tends to 0 (the logarithm of q tends to -∞), the PCM is fully liquid and the thermal storage is affected only the sensible heat but with respect to the first stage the temperature difference is very small.

Effect of porosity

Figs.12-14 illustrate the effect of porosity on the physical quantity in the LTE. When the porosity increases, the thermal performance parameter q raises in the steady stage where the latent heat is predominant respect to sensible heat. The temperature presents the same behaviour of q but the growth towards the isothermal value is slower. Increasing the porosity the liquid fraction has slower growth because of the growth of temperature is slower for the higher porosity values.

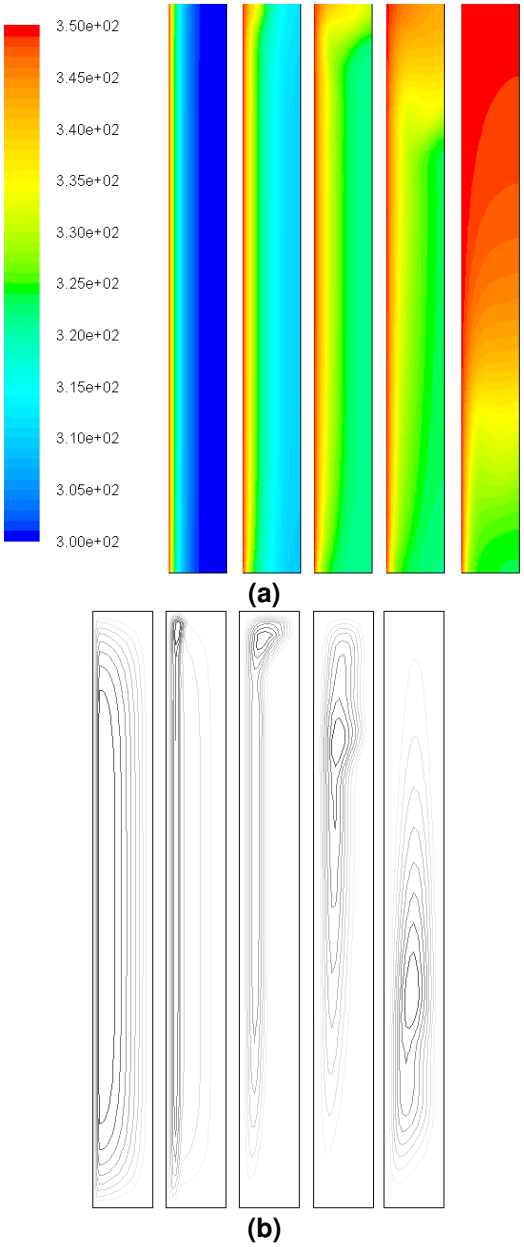

FIGURE 7 TEMPERATURE FIELD (A) AND STREAM FUNCTION (B) FOR DIFFERENT TIME VALUES, 30 s, 300 s, 900 s, 1500 s, 3000 s

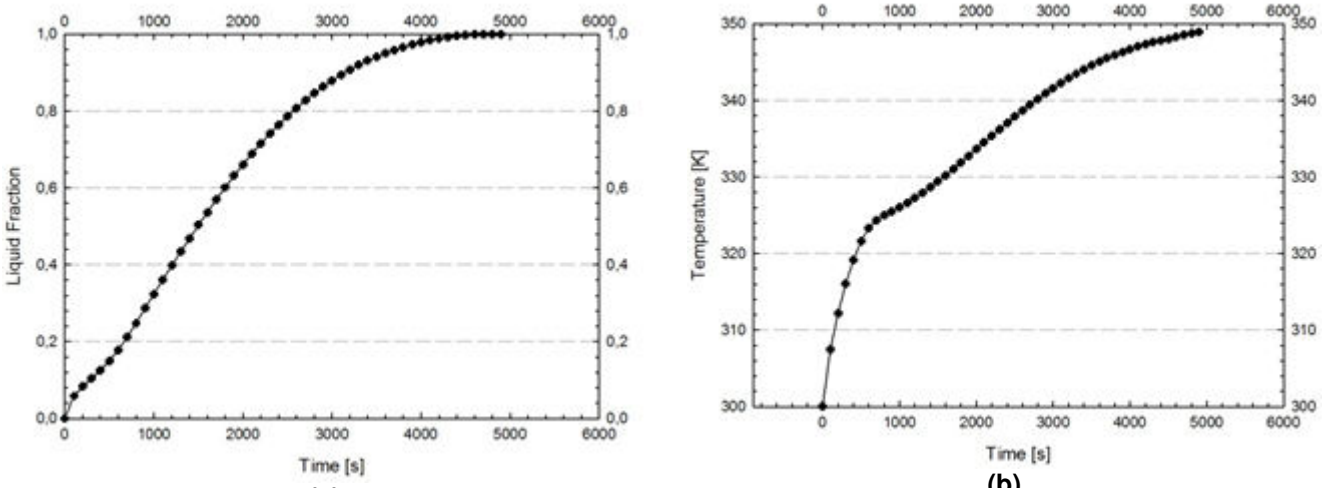

(a) (b)

FIGURE 8. AVERAGE VALUES OF: (A) LIQUID FRACTION AND (B) TEMPERATURE PROFILES IN CLEAN CASE.

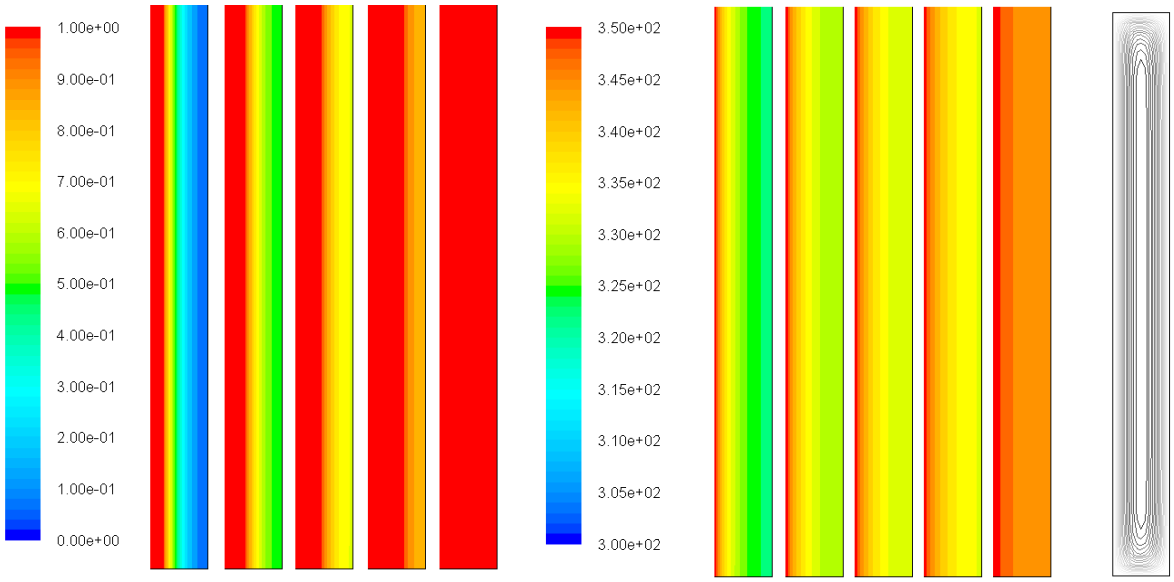

(a) (b) (c)

FIGURE 9 RESULTS FOR PCM IN METAL FOAM WITH A POROSITY EQUAL TO 0.80 AND 20 PPI FOR DIFFERENT TIMES EQUAL TO 5 s, 10 s, 12.5 s, 15 s, 20 s: (A) LIQUID FRACTION FIELD; (B) TEMPERATURE FIELD AND (C) STREAM FUNCTION FIELD.

The reason for which the porosity influences the behaviour of the temperature can be explain by means of the analysis of effective thermal conductivity as a function of porosity. In fact, when the porosity arises, the conductivity decreases as observed in Fig. 15. The heat conduction is predominant with respect to the convection and, consequently, it is required more time to reach the isothermal value for higher porosity.

These observations are the same for the LTNE model, but the values related to the temperature, liquid fraction and thermal performance parameter q are different. A way to compare the LTE and LTNE models is to plot the melting time for these two models. Fig. 16 shows the differences between the two models in terms of melting time. In particular, the melting time increases when the porosity is higher but the LTNE model presents a higher value for lower porosity values while for higher porosity values both models tend to reach the same value. The interpretation of this behavior is deduced by term $\alpha_{sf}h_{sf}$ that links the equation of energy for PCM, Eq. (9), to the energy equation for metal foam, Eq. (10) because when the porosity is higher this term tends to increase and the temperature gradients between metal foam and PCM are reduced.

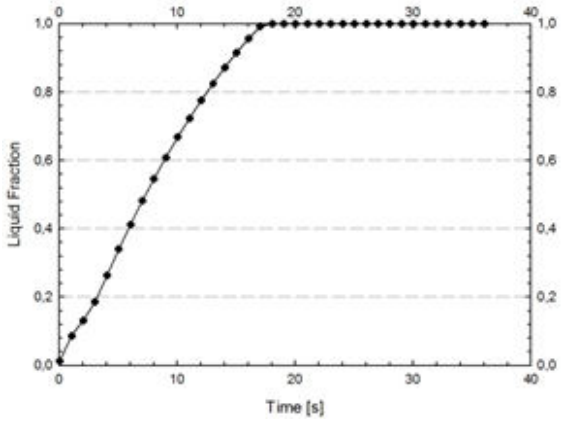

(a)

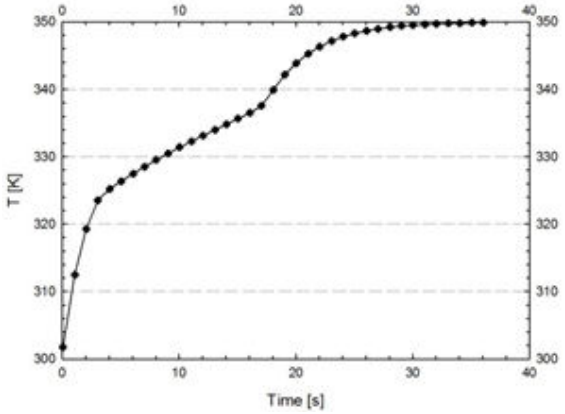

(b)

FIGURE 10. MEAN VALUES OF: (A) LIQUID FRACTION AND (B) TEMPERATURE AS FUNCTIONS OF TIME FOR THE CASE PCM IN METAL FOAM WITH A POROSITY EQUAL TO 0.80 AND 20 PPI.

CONCLUSIONS

Thermal behaviors in a latent heat thermal energy storage (LHTSS) with pure phase change material (PCM) or PCM in aluminum foams was performed by a numerical analysis. The investigation was carried out modeling phase change process with enthalpy-porosity method and the aluminum foam was considered as a porous media under the assumption of Darcy-Forchheimer law and local thermal equilibrium or local thermal non equilibrium. Numerical simulations were obtained for a vertical shell and tube LHTES made with two concentric aluminum tubes. Results in terms of liquid fraction, temperature and stream function fields for different time values were presented and average liquid fraction, system temperature and thermal performance parameter profiles as functions of time were evaluated and analyzed for the cases without and with aluminum foam. In the last case the effect of porosity was examined. The presence of aluminum foam determined a significant reduction of the melting time of about two order of magnitude and the conduction was the dominant mechanism in the PCM melting. The porosity increase determined an increase in the melting time due to the decrease of effective thermal conduction of the PCM with the aluminum foam. Moreover, the comparison between the LTE and LTNE models indicated that the melting time in the LTNE is greater than the one in the LTE. The presence of metal foam improves significantly the heat transfer in the LHTES giving a very faster phase change process with respect to pure PCM. In addition, this numerical investigation can be further enlarged to simulate different types of metal foam and PCM.

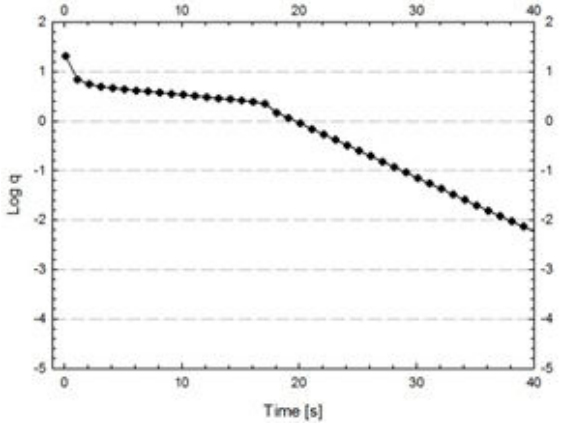

FIGURE 11 LOG q AS FUNCTION OF TIME

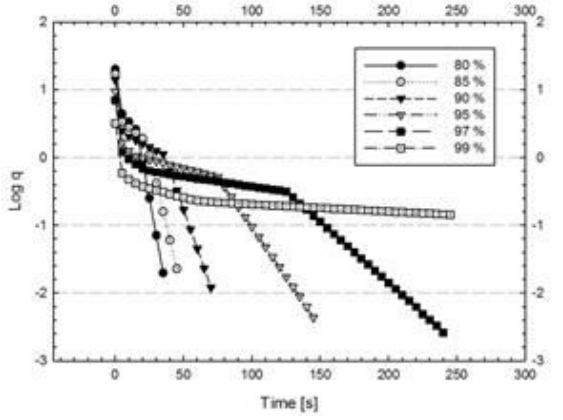

(a)

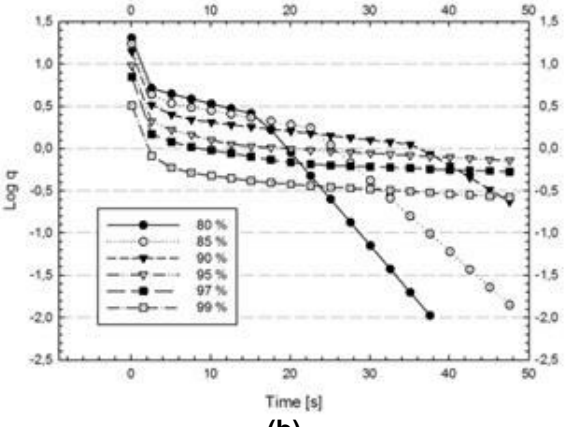

(b)

FIGURE 12 LOG q: (A) AS FUNCTION OF TIME AND (B) AT THE FIRST 50 s.

NOMENCLATURE

T	temperature	K
$T_{solidus}$	solidus temperature	K
$T_{liquidus}$	liquidus temperature	K
T_{wall}	wall temperature	K
V,$\vec{V}$	vector velocity	ms^{-1}
p	pressure	Pa
g,$\vec{g}$	gravity acceleration	ms^{-2}
$\vec{S}$	source term	eq. (4-5)
A_{mush}	mushy zone costant	$kgm^{-3}s^{-1}$
K	permeability	m^2
C_F	inertial drag factor	eq. (5)
c	specific heat	$Jkg^{-1}K^{-1}$
k	thermal conductivity	$Wm^{-1}K^{-1}$
H_L	latent Heat of PCM	Jkg^{-1}
t	time	s
h_{sf}	local heat transfer coefficient	$Wm^{-2}K^{-1}$
L	characteristic length	m
Re_d	ligament Reynolds number	eq. (17)
Pr	Prandtl number	eq. (17)
d_f	ligament diameter	m
d_p	pore diameter	m
q	performance parameter	eq. (19)
E	specific enthalpy	Jkg^{-1}
Δt	time step	s

Greek Symbols

β	liquid fraction	Eq. (1)
ρ	density	kgm^{-3}
γ	thermal expansion coefficient	K^{-1}
μ	viscosity of PCM	$kgm^{-1}s^{-1}$
π	costant number	eq. (5)
ε	porosity	
α_{sf}	surface Area density	m^{-1}
ω	pore size	Pore per Inch (PPI)

subscripts

0	operating
pcm	phase change material
m	metal foam
eff	effective

REFERENCES

[1] Antoni, G., Marc, M., Ingrid, M., Ana, L. , Pablo, D., Belén, Z., Luisa, F. C., 2010 "State of the art on high temperature thermal energy storage for power generation. Part 1 – Concepts, materials and modellization", Renewable and Sustainable Energy Reviews, **14**, pp. 31-55.

[2] Zhou, D., Zhao, C.Y.,Tian, Y., 2012, "Review on thermal energy storage with phase change materials (PCMs) in building applications", Applied Energy, **92**, pp. 593-605.

[3] Cabeza, L. F.,2014, "Advances in Thermal Energy Storage Systems: Methods and Applications", Woodhead Publishing Series in Energy,

[4] Dell, R., Rand, D., 2001, "Energy storage a key technology for global energy sustainability", Journal of Power Sources, **100**, pp. 2-17.

[5] Beckmann, G. and Gilli, P.V., 2002 Thermal Energy Storage: Basics, Design, Applications to Power Generation and Heat Supply, Springer, Vienna.

[6] Paksoy, H.Ö., 2007, Thermal Energy Storage for Sustainable Energy Consumption: Fundamentals, Case Studies and Design, Springer, Berlin.

[7] Arteconi, A., Hewitt, N.J., Polonara, F., 2012, "State of the art of thermal storage for demand-side management", Applied Energy, **93** , pp. 371-389.

[8] Oró, E., Gil, A.,de Gracia A., Boer, D., Cabeza, L.F., 2012, "Comparative life cycle assessment of thermal energy storage systems for solar power plants", Renewable Energy, **44**, pp. 166-173.

[9] Dincer, I. and Rosen,M., 2010, Thermal Energy Storage: System and Application, 2nd ed., John Wiley & Sons, New York.

[10] Kalaiselvam, S. and Parameshwaran, R., 2014 Thermal Energy Storage Technologies for Sustainability: Systems Design, Assessment and Applications Paperback – August 22, Academic Press; 1 edition 2014.

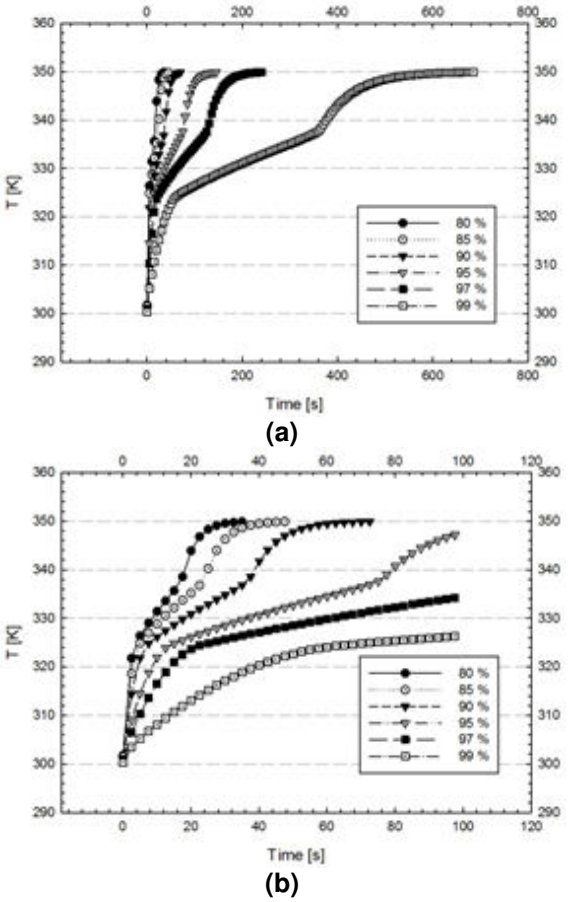

FIGURE 13. TEMPERATURE: (A) AS FUNCTION OF TIME AND (B) AT THE FIRST 100 s.

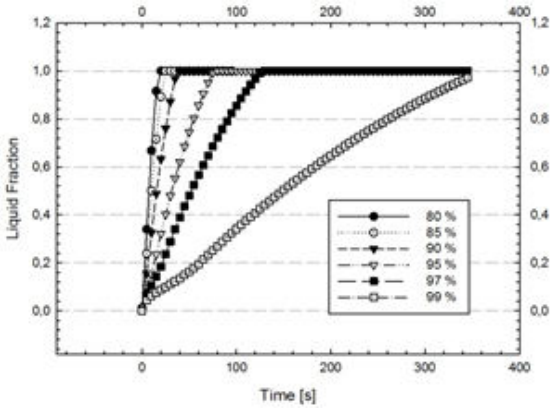

(a)

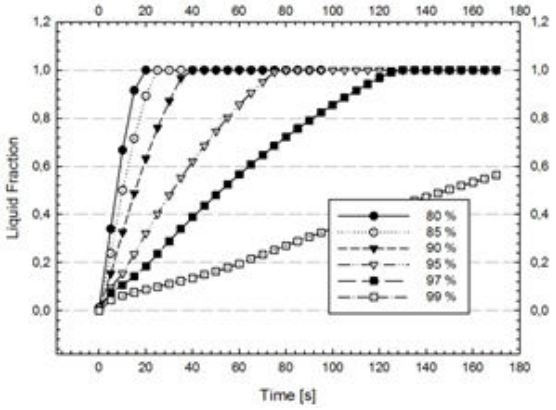

(b)

FIGURE 14. LIQUID FRACTION: (A) AS FUNCTION OF TIME AND (B) AT THE FIRST 200 s.

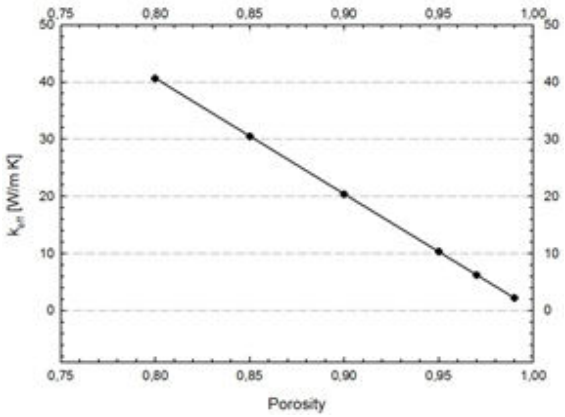

FIGURE 15. EFFECTIVE THERMAL CONDUCTIVITY OF THE WHOLE SYSTEM VS POROSITY.

[11] Shao, J., Darkwa, J., Kokogiannakis, G.,2015, "Review of phase change emulsions (PCMEs) and their applications in HVAC systems", Energy and Buildings, **94**, pp. 200-217.

[12] Sharma, R.K., Ganesan, P., Tyagi, V.V., Metselaar, H.S.C., Sandaran, S.C., 2015 "Developments in organic solid-liquid phase change materials and their applications in thermal energy storage", Energy Conversion and Management, **95**, pp. 193-228.

[13] Heier, J., Bales, C., Martin, V., 2015, "Combining thermal energy storage with buildings - A review", Renewable and Sustainable Energy Reviews, **42**, pp. 1305-1325

[14] Cabeza, L.F., Gutierrez, A., Barreneche, C., Ushak, S., Fernández, A.G., Inés Fernádez, A., Grágeda, M., 2015, "Lithium in thermal energy storage: A state-of-the-art review" , Renewable and Sustainable Energy Reviews, **42**, pp. 1106-1112.

[15] Pintaldi, S., Perfumo, C., Sethuvenkatraman, S., White, S., Rosengarten, G., 2015, "A review of thermal energy storage technologies and control approaches for solar cooling", Renewable and Sustainable Energy Reviews, **41**, pp. 975-995.

[16] Hesaraki, A., Holmberg, S., Haghighat, F., 2015, "Seasonal thermal energy storage with heat pumps and low temperatures in building projects - A comparative review" , Renewable and Sustainable Energy Reviews, **43**, pp. 1199-1213.

[17] Gude, V.G.,2015, "Energy storage for desalination processes powered by renewable energy and waste heat sources", Applied Energy, **137**, pp. 877-898.

[18] Sabihuddin, S., Kiprakis, A.E., Mueller, M.,2015, "A numerical and graphical review of energy storage technologies, Energies, **8**, pp. 172-216.

[19] Yan, T., Wang, R.Z., Li, T.X., Wang, L.W., Fred, I.T., 2015, "A review of promising candidate reactions for chemical heat storage" Renewable and Sustainable Energy Reviews, **43**, pp. 13-31.

[20] Fulpagare, Y., Bhargav, A.,2015 "Advances in data center thermal management", Renewable and Sustainable Energy Reviews, **43**, pp. 981-996.

[21] Aydin, D., Casey, S.P., Riffat, S.,2015, "The latest advancements on thermochemical heat storage systems" Renewable and Sustainable Energy Reviews, **41**, pp. 356-367.

[22] Muñoz-Criollo, J.J., Cleall, P.J., Rees, S.W.,2015, "Impacts of surface fluxes on inter-seasonal heat storage in soils", First Break, **33 (1)** , pp. 45-50.

[23] Abhat A.,1983, "Low temperature latent heat thermal energy storage: heat storage materials", Solar Energy, **30**, pp.313-332.

[24] Zhang Y, Faghri A., 1996, "Heat transfer enhancement in latent heat thermal energy storage system by using the internally finned tube", Journal of Enhanced Heat Transfer, **3**, pp. 119-127.

[25] Zhao, C. Y. ,Lu, W., Tian,Y.,2010, "Heat transfer enhancement for thermal energy storage using metal foams embedded within phase change materials (PCMs)", Solar Energy, **84**, pp. 1402-1412.

[26] Yang, Y. Y.,Luo, L., Song, G. L., Liu, Y.,Tang, G.,2014, "The experimental exploration of nano-Si_3N_4/paraffin on thermal behavior of phase change materials", Thermochimica Acta **597**, pp. 101-106.

[27] Dukhan, N., 2013, Metal Foams: Fundamentals and Applications, DEStech Publications, Inc, Lancaster.

[28] Krishnan, S., Murthy, J.Y., Garimella, S.V., 2005. "A two-temperature model for solid–liquid phase change in metal foams", ASME Journal of Heat Transfer, **127**, pp. 995–1004.

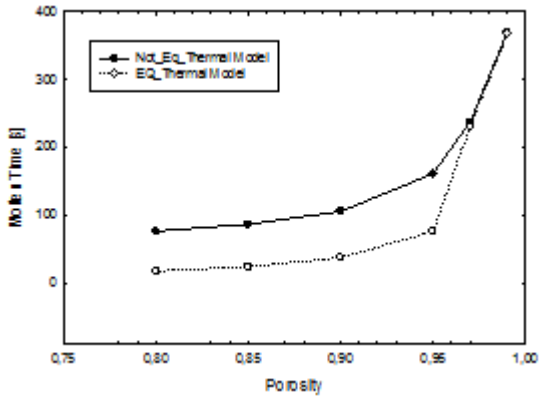

FIGURE16. MOLTEN TIME VS POROSITY FOR LTE AND LTNE MODELS.

[29] Siahpush, A., O'Brien, J., Crepeau, J., 2008, "Phase change heat transfer enhancement using copper porous foam", ASME Journal of Heat Transfer, **130**, art. no. 082301.

[30] Zhou, D., Zhao,C.Y., 2011, "Experimental investigations on heat transfer in phase change materials (PCMs) embedded in porous materials", Applied Thermal Engineering, **31**, pp. 970-977.

[31] Tian, Y., Zhao, C.Y., 2011, "A numerical investigation of heat transfer in phase change materials (PCMs) embedded in porous metals", Energy, **36**, pp. 5539-5546.

[32] Zhao, C.Y., Wu, Z.G., 2011, "Heat transfer enhancement of high temperature thermal energy storage using metal foams and expanded graphite", Solar Energy Materials and Solar Cells, **95**, pp. 636-643.

[33] Cui, H.T., 2012, "Experimental investigation on the heat charging process by paraffin filled with high porosity copper foam", Applied Thermal Engineering, **39**, pp. 26-28.

[34] Yang, J., Du, X., Yang, L., Yang, Y.,2013, "Numerical analysis on the thermal behavior of high temperature latent heat thermal energy storage system", Solar Energy, **98**, pp. 543-552.

[35] Liu, Z., Yao, Y., Wu, H.,2013, "Numerical modeling for solid–liquid phase change phenomena in porous media: Shell-and-tube type latent heat thermal energy storage", Applied Energy, **112**, pp.1222–1232.

[36] Sundarram, S.S., Li, W., 2014 "The effect of pore size and porosity on thermal management performance of phase change material infiltrated microcellular metal foams", Applied Thermal Engineering, **64**, pp. 147-154.

[37] Zhang, H.L., Baeyens, J., Degrève, J., Cáceres, G., Segal, R., Pitié, F.,2014, "Latent heat storage with tubular-encapsulated phase change materials (PCMs)", Energy, **76**, pp. 66-72.

[38] Chen, Z., Gao, D., Shi J.,2014, "Experimental and numerical study on melting of phase change materials in metal foams at pore scale", International Journal of Heat and Mass Transfer, **72**, pp. 646–655.

[39] Xiao, X., Zhang, P.,Li, M.,2014 "Effective thermal conductivity of open-cell metal foams impregnated with pure paraffin for latent heat storage", International Journal of Thermal Sciences, **81**, pp.84-105.

[40] Li, W.Q., Qu, Z.G., He, Y.L., Tao, Y.B.,2014, "Experimental study of a passive thermal management system for high-powered lithium ion batteries using porous metal foam saturated with phase change materials", Journal of Power Sources, **255**, pp. 9-15.

[41] Srivatsa, P.V.S.S., Baby, R., Balaji, C.,2014, "Numerical investigation of PCM based heat sinks with embedded metal foam/crossed plate fins", Numerical Heat Transfer; Part A: Applications, **66**, pp. 1131-1153.

[42] Zhang, P., Xiao, X., Meng, Z.N., Li, M., 2015, "Heat transfer characteristics of a molten-salt thermal energy storage unit with and without heat transfer enhancement", Applied Energy, **137**, pp. 758-772.

[43] Wang, Z., Zhang, Z., Jia, L., Yang, L.,2015, "Paraffin and paraffin/aluminum foam composite phase change material heat storage experimental study based on thermal management of Li-ion battery", Applied Thermal Engineering, **78**, pp. 428-436.

[44] Yang, J., Yang, L.,Xu, C., Du, X. ,2015, "Numerical analysis on thermal behavior of solid–liquid phase change within copper foam with varying porosity", International Journal of Heat and Mass Transfer **84** ,pp. 1008–1018.

[45] Tasnim, S.H., Hossain, R., Mahmud, S., Dutta, A., 2015, "Convection effect on the melting process of nano-PCM inside porous enclosure", International Journal of Heat and Mass Transfer, **85**, pp. 206-210.

[46] Yilbas, B.S., Shuja, S.Z., Shaukat, M.M.,2015, "Thermal characteristics of latent heat thermal storage: Comparison of aluminum foam and mesh configurations", Numerical Heat Transfer; Part A: Applications, **68**, pp. 99-116.

[47] Voller, V. R., Prakash, C.,1987, "A fixed grid numerical modelling methodology for convection-diffusion mushy region phase-change problems", International Journal of Heat and Mass Transfer, **30**, pp.1709-1719

[48] Al-abidi, A. , Bin Mat, S. , Sopian, K., Sulaiman, M.Y., Mohammed, A. Th., 2013, "CFD application for latent heat thermal energy storage: a review", Renewable and Sustainable Energy Reviews, **20**, pp. 353-363.

[49] Nithyanandam, K., Pitchumani, R., 2014, "Computational studies on metal foam and heat pipe enhanced latent thermal energy storage", Journal of Heat Transfer, **136**, 051503.

[50] Boomsma, K., Poulikakos, D., 2001, "On the Effective Thermal Conductivity of a Three-Dimensionally Structured Fluid-Saturated Metal Foam", International Journal Heat Mass Transfer, **44**, pp. 827-836.

[51] Rubitherm GmBH, www.rubitherm.de.

[52] Calmidi, V.V., and Mahajan, R.L., 2000, "Forced Convection in High Porosity Metal Foams", ASME Journal Heat Transfer, 122, pag. 557-565.

[53] Zukauskas, A.A., 1987, Handbook of Single-phase Heat Transfer, "S. Kakac and R.K. Shah, ed. Wiley-Interscience, New York.

[54] Ansys Incorporated, *Fluent 15.0 User Manual*, 2014.